J. Fluid Mech. (1989), *vol.* 206, *pp.* 563–578
Printed in Great Britain

Experimental study of bore run-up

By HARRY H. YEH, ABDULHAMID GHAZALI AND INGUNN MARTON

Department of Civil Engineering, FX-10, University of Washington, Seattle, WA 98195, USA

(Received 29 February 1988 and in revised form 22 November 1988)

Bore propagation near the shoreline, the transition from bore to wave run-up, and the ensuing run-up motion on a uniformly sloping beach are investigated experimentally. As a bore approaches the shoreline, the propagation speed first decelerates by compressing its wave form and then suddenly accelerates at the shoreline. Although this behaviour is qualitatively in agreement with the inviscid shallow-water wave prediction (often called the 'bore collapse' phenomenon), unlike the genuine bore-collapse phenomenon, the acceleration is caused by the 'momentum exchange' process, i.e. collision of the bore against the initially quiescent water along the shoreline. Owing to this momentum exchange, a single bore motion degenerates into two successive run-up water masses; one involves a turbulent run-up water motion followed by the original incident wave motion. The transition process from undular bore to wave run-up appears to be different from that of a fully developed bore. The bore front overturns directly onto the dry beach surface, and the run-up is characterized by a thin splashed-up flow layer.

1. Introduction

A bore and the ensuing run-up on a uniformly sloping beach have been analysed based on the inviscid theory with the assumption of a hydrostatic pressure field, i.e. the shallow-water wave theory. For a two-dimensional problem (no longshore variation) as shown in figure 1, the depth-integrated conservation equations of mass and momentum are found, respectively, to be

$$\frac{\partial \eta}{\partial t}+\frac{\partial}{\partial x}\{(\eta+h)\,u\}=0, \tag{1}$$

$$\frac{\partial u}{\partial t}+u\frac{\partial u}{\partial x}+g\frac{\partial \eta}{\partial x}=0, \tag{2}$$

where the x-coordinate points in the inshore direction from the shoreline, $u(x,t)$ is the depth-integrated water particle velocity, $\eta(x,t)$ is the departure of the water surface from the quiescent water depth $h(x)$, and g is the acceleration due to gravity. A bore front is usually treated by the jump conditions, i.e. the conservation of mass and momentum at the mathematical discontinuity:

$$u=\frac{U\eta}{(\eta+h)}, \tag{3}$$

$$U^2=\frac{g(\eta+h)\,(\eta+2h)}{2h}, \tag{4}$$

where $U(x,t)$ is the bore front velocity.

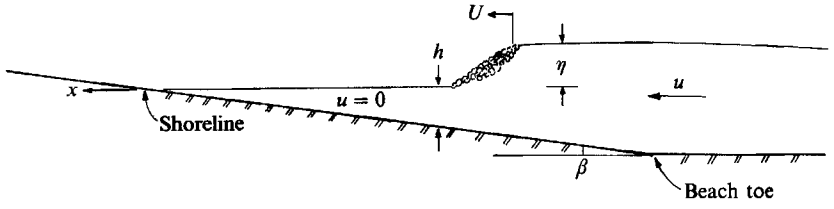

FIGURE 1. Definition sketch.

To solve the above mathematical problem of bore propagation on a plane beach, Whitham (1958) proposed an approximate solution method called the characteristic rule. The method is to solve the exact differential relation,

$$\mathrm{d}u+2\mathrm{d}c-g\frac{\mathrm{d}h}{(u+c)}=0, \tag{5}$$

valid on the advancing characteristic line $\mathrm{d}x/\mathrm{d}t=u+c$, where $c=(g(h+\eta))^{\frac{1}{2}}$. By substituting the jump conditions (3) and (4) into (5), Whitham found that

$$\frac{1}{h}\frac{\mathrm{d}h}{\mathrm{d}M}=\frac{-4(M+1)(M-\frac{1}{2})^2(M^3+M^2-M-\frac{1}{2})}{(M-1)(M^2-\frac{1}{2})(M^4+3M^3+M^2-\frac{3}{2}M-1)}, \tag{6}$$

where $M=U/c$. Keller, Levine, & Whitham (1960) and Ho & Meyer (1962) demonstrated that Whitham's characteristic rule provides an accurate solution. Based on their analyses (Whitham 1958; Keller *et al.* 1960; Ho & Meyer 1962), the shallow-water wave theory predicts that the height of a bore tends to vanish as it approaches the shoreline. At the shoreline, the fluid velocity, u, and bore front velocity, U, approach their common finite value, U^*, whereas their accelerations become singular at the shoreline. This behaviour at a shoreline involving the rapid conversion of potential to kinetic energy is often called 'bore collapse'.

The experimental results of Yeh & Ghazali (1986, 1988) demonstrated the detailed transition process at the shoreline. Based on their results, the transition process was found to involve the 'momentum exchange' between the bore and the small wedge-shaped water body along the shore. As shown in figure 2, the bore front itself does not reach the shoreline directly, but the bore pushes a small initially quiescent mass of water in front of it. The term 'momentum exchange' is used here to describe this transition since the process is analogous to the collision of two bodies; a fast-moving large mass (i.e. bore) collides with a small stationary mass (the wedge-shaped water mass along the shoreline). Yeh & Ghazali (1986, 1988) also found that the turbulence on the front face of a bore, as well as that generated at the transition process, is advected forward onto the dry beach with the run-up motion instead of being left behind the wave front.

Based on the shallow-water wave theory, Shen & Meyer (1963) analysed the wave run-up which subsequently occurs after the bore collapse. They found that the motion of a run-up front is totally governed by the gravity force. Hence, the run-up front velocity can be expressed as

$$U=\frac{\mathrm{d}x_{\mathrm{s}}}{\mathrm{d}t}=(U^{*2}-2\gamma x_{\mathrm{s}})^{\frac{1}{2}}, \tag{7}$$

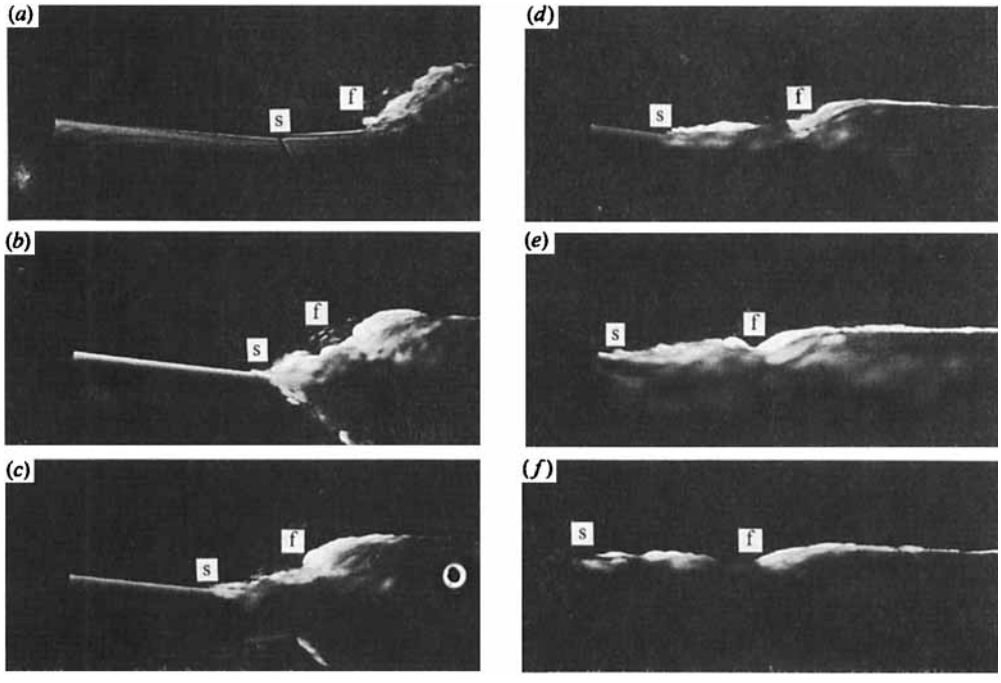

FIGURE 2. Transition process from bore to run-up mode. Initial Froude number, $F = 1.43$. (*a*) Bore approaching the shore, (*b* – *e*) transition, (*f*) run-up. f, bore front; s, run-up wave tip (after Yeh & Ghazali 1988).

where $x_s(t)$ is the position of the run-up front, and $\gamma = g\beta$, β being the beach slope from the horizontal. Hence, the maximum run-up height, R, is simply

$$R = \frac{U^{*2}}{2g}, \tag{8}$$

which is a total conversion of kinetic energy at the bore collapse to potential energy. Shen & Meyer (1963) found that the water depth close to the front can be approximated by

$$h(x,t) \to \frac{(x_s(t)-x)^2}{(3t)^2}, \tag{9}$$

as $(x_s - x) \to 0$. According to (9), the water surface is tangential to the beach surface at the front and the sheet of run-up becomes thinner as time increases.

The entire process of bore propagation, run-up and drawdown was numerically simulated by Hibberd & Peregrine (1979); the inviscid shallow-water wave equations (1) and (2), were solved using the Lax–Wendroff numerical technique without imposing jump conditions. Their predictions of the maximum run-up heights appeared to be in good agreement with the analytical prediction, (8). Nonetheless, the analytical and numerical predictions of the maximum run-up height are considerably greater than the experimental results measured by Miller (1968). Packwood & Peregrine (1981) extended Hibberd & Peregrine's (1979) numerical model by incorporating viscous effects with the Chézy friction term. While good agreement with Miller's (1968) experimental results were obtained for the steep-

beach condition ($\beta = 15°$), for the mild-slope condition ($\beta = 2°$) the friction effects alone cannot be the explanation for the discrepancy in the maximum run-up heights, i.e. the numerical predictions of the viscous model still considerably exceeds Miller's experimental results.

Svendsen & Madsen (1984) modified the inviscid shallow-water wave theory to include turbulence effects by applying the k–ϵ turbulence model. A similarity profile of the flow velocity in the turbulent region was assumed based on Madsen & Svendsen's (1983) data on hydraulic jump. While Svendsen & Madsen's (1984) model cannot be extended for analyses of the transition of bore to run-up mode nor the ensuing wave run-up, the model is able to provide information about the shape and structure of the front. According to Svendsen & Madsen, as the bore front approaches the shore, the front becomes less steep and decelerates, but moves faster than the speed predicted in Hibberd & Peregrine's (1979) model. This is caused by enhancement of the momentum flux behind the front due to the non-uniform velocity profile, which is modelled in Svendsen & Madsen's (1984) model but not in Hibberd & Peregrine's model. The experimental observations of Yeh & Ghazali (1986, 1988) indicate that turbulence generated at the bore front is sporadic and three-dimensional, while Svendsen & Madsen's numerical results appear to form a much thicker and distinct turbulent region. However, a direct comparison may not be made because the beach slopes considered are different; Svendsen & Madsen used $\beta = 1.66°$ whereas the experiments by Yeh & Ghazali (1986, 1988) were performed with $\beta = 7.5°$.

As mentioned earlier, extensive laboratory experiments were performed by Miller (1968) who reported the maximum run-up heights for a variety of bore strengths and beach slopes ($\beta = 2°$ to $15°$). Miller used a flat vertical piston to generate the bores; the piston was impulsively started and moved at a constant speed over a finite distance and suddenly stopped at the end. Packwood & Peregrine (1981) pointed out that when the piston stops, a simple depression wave was generated. Although, for the inviscid model, the characteristics from this depression wave do not catch up with the moving run-up front, Packwood & Peregrine showed that Miller's run-up results of actual (viscous) flow on mild slopes are influenced by this depression wave.

In the present study, we investigate experimentally the behaviour of bore near the shoreline and the ensuing run-up process. The aim of the study is to identify the shortcomings of, or to verify, the shallow-water wave theory, and to elucidate the detailed physics involved in the wave run-up.

2. Experiment

A series of experiments was performed in a 9.0 m long, 1.2 m wide, and 0.9 m deep wave tank as shown in figure 3. (The same experimental facility was used by Yeh & Ghazali 1986, 1988.) A single bore is generated by lifting the 12.7 mm thick aluminium plate gate which initially separates the quiescent water on the beach from the deeper water behind the gate. One advantage of this bore-generation scheme is that the theoretical prediction of the bores can be made without difficulty from the classic dam-break problem. Furthermore, the depression wave that initially propagates offshore and is then reflected back at the endwall does not influence the flow during the run-up process. The gate is lifted with the aid of a pneumatic cylinder (10.2 cm bore diameter) which is electrically activated by a single solenoid valve with the operating air pressure of 650 kPa, i.e. the maximum lifting force is 5.3 kN. The system is capable of lifting 20 cm of the gate travel distance in 0.0708 ± 0.0012 s.

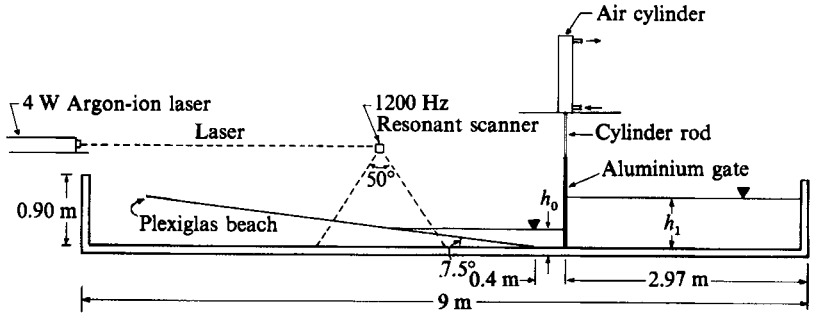

FIGURE 3. A schematic view of the experimental apparatus.

Hence, bores can be generated by almost instantaneous openings of the gate in a repeatable manner ($\pm 1.7\%$ error). The distance from the gate to the shoreline is 114 cm, which is approximately a propagation distance of $20\eta_0$ where η_0 is a typical bore height offshore in the horizontal-bottom region. The tank width is 120 cm, hence the sidewall effects should be negligible for the experimental data obtained along the centreline of the tank.

The bore-generating system was tested with a variety of initial conditions. It was visually observed that fully developed bores can be generated when $h_1/h_0 > 2.0$, where h_0 and h_1 are the initial water depths in front of and behind the gate, respectively. In the case of $h_1/h_0 < 2.0$, the generated bores were undular (although the leading wave is breaking at its crest when $1.6 < h_1/h_0 < 2.0$); this is because linear effects of frequency dispersion become significant in comparison with the nonlinear effects. On the other hand, when $h_1/h_0 > 2.8$, the behaviour of generated bores appeared to be too transient for the measurements. This must be due to the limited propagation distance available and the finite time involved in lifting up the gate, i.e. there is insufficient time for the bore to develop before it reaches the shore. Nonetheless, for bores generated with $2.0 < h_1/h_0 < 2.6$, the propagation distance appears long enough to form a fully developed bore on the beach.

The theory provided by Ho & Meyer (1962) followed by Ho, Meyer & Shen (1963) indicates that, just before the bore reaches the shoreline, the final bore behaviour is virtually independent of the detailed initial wave condition offshore. In other words, bores created by any initial conditions behave qualitatively the same near the shoreline; the only important parameter which influences the strength of bore nearshore is the value of U^* (i.e. the terminal velocity at the shoreline, which is also a measure of the energy at the initial time). According to this shallow-water wave theory, as long as a fully developed bore is generated offshore, the limited bore propagation distance available to our experiments should not be a significant drawback to the study of a bore nearshore and the ensuing run-up process: hence, the experimental results should be considered to be general, and not limited to this particular experimental set-up. However, this is not the case in the laboratory experiments. In a real fluid environment, dispersion effects are always present, and the bore front is not a discontinuity but has a finite length. Even though our bore-generating system opens the gate almost instantaneously, the fluid must first accelerate both vertically downward and horizontally forward to form a bore. This initial vertical acceleration generates waves of finite length which might contaminate the 'uniform' bore with a limited propagation distance; with a long propagation distance, those waves would disperse and separate from the bore front. This

limitation of the experiments (or theory) might be of some importance and is considered in the theoretical and experimental comparisons described in §3.

A 4-W Argon-ion laser is used for the visualization of a bore profile. The emitted laser beam is converted to a thin sheet of laser light through a resonant scanner. The scanner is capable of sweeping the beam at 1200 Hz with a maximum of a 50° peak-to-peak angle. The generated laser sheet is projected from above in the cross-shore direction along the centreline of the tank. This illuminates the vertical longitudinal plane of the water dyed with fluorescein. This type of flow visualization is often called the laser-induced fluorescence method.

Velocities of bore propagation are measured by an array of water sensors, with a sampling rate of 1250Hz, along the centreline of the tank. In the offshore region, the water sensors were placed from above 5 cm apart; each sensor tip was placed approximately 1 mm above the initial quiescent water level. An attempt was made to use the same method to measure the velocities of the run-up tip on the beach. A difficulty arose with the formation of a very thin sheet of run-up water: the flow disturbance caused by a sensor rod (1.6 mm in diameter) influences the adjacent sensor. To minimize this difficulty, the run-up velocities were measured by an array of sensors embedded in the beach. The sensor tip projected no more than 1 mm above the beach surface.

The flow structures near the maximum run-up were recorded from above by an 8 mm video camcorder and a 35 mm photo camera. The maximum run-up heights were directly measured from the video images.

3. Results

3.1. *Fully developed bore*

The laser-induced fluorescence method was adopted to measure the bore profile in the longitudinal plane. Because the laser sheet is approximately 1 mm thick, the method can provide flow visualization in a virtually two-dimensional plane. A typical image of the bore is shown in figure 4. The location of the front toe is $x = -9$ cm (the x-coordinate points inshore from the initial shoreline) and the initial water depth offshore in the horizontal-bottom region, h_0, is 9.75 cm. The initial strength of this bore can be represented by the offshore Froude number, $F = U_0/(gh_0)^{\frac{1}{2}} = 1.43$ (or $h_1/h_0 = 2.31$), where U_0 is the bore propagation speed offshore in the horizontal-bottom region. (The value of U_0 was computed from the classic dam-break problem.) This offshore bore strength of $F = 1.43$ is comparable to the $F = 1.45$ and 1.37 used in the numerical studies by Hibberd & Peregrine (1979) and Svendsen & Madsen (1984), respectively. It is noted that the initial bore strength in a natural beach is limited due to the wave breaking mechanism, and the value of $F \approx 1.4$ seems to be typical according to the results provided by Svendsen, Madsen & Hansen (1978).

The profile of figure 4 clearly indicates that the bore is fully developed, i.e. the entire front face is turbulent, but unlike numerical predictions based on the shallow-water wave theory, the bore elevation is not spatially uniform but forms a distinct 'head' at the front. The reason is unclear but the head-formation feature may be caused by linear effects of frequency dispersion. The shallow-water wave theory cannot predict a local feature of the profile near the front where the vertical motion is important. In addition, as discussed in §2, waves of finite length generated at the gate might influence this offshore feature of the bore; such waves would disperse and separate from the bore front in a sufficiently long distance but not in the limited propagation distance available to our experimental facility.

Because of the head formation, it is difficult to define the bore height, η. In figure

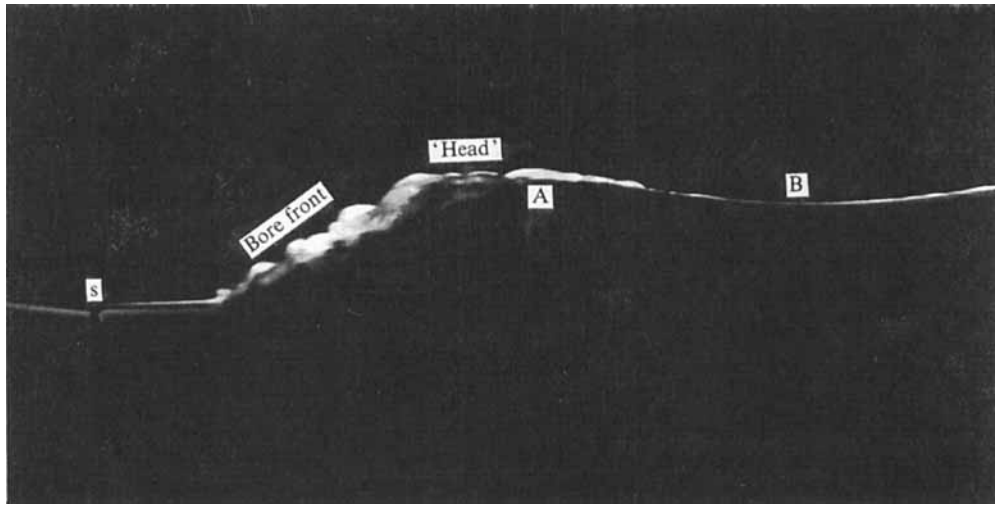

FIGURE 4. A longitudinal bore profile illuminated by the laser sheet. A, the maximum bore height at the head; B, the uniform height behind the head; s, the shoreline. Initial Froude number, $F = 1.43$. The toe of the bore front is at $x = -9$ cm.

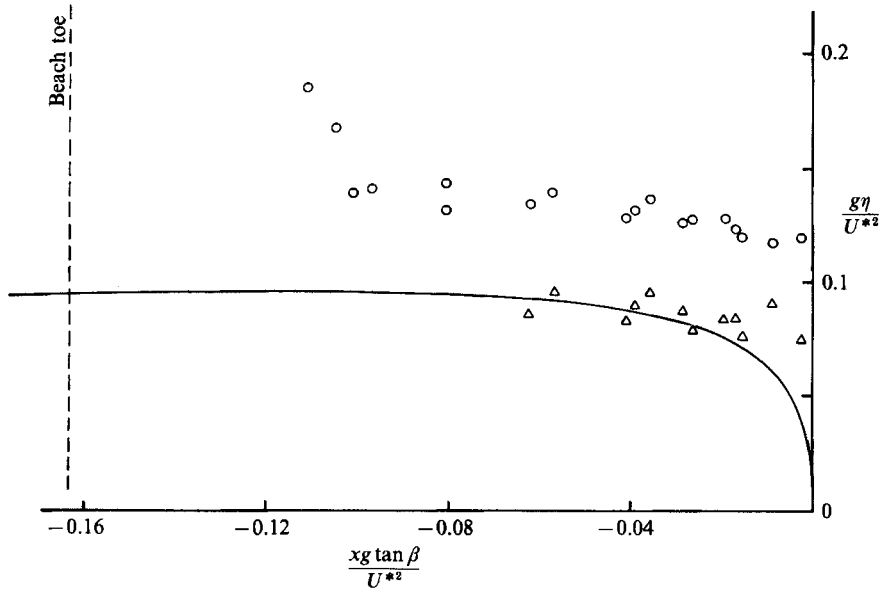

FIGURE 5. Offshore bore-height variation. Initial Froude number, $F = 1.43$;,○ height of the bore head; △, height behind the head; ——, theoretical prediction by Ho & Meyer (1962).

5, the maximum height at the head (indicated by the point A in figure 4), and the uniform height behind the head (indicated by the point B in figure 4) are plotted against the bore location; the bore location is defined as that at the front toe. The theoretical prediction based on Ho & Meyer's (1962) work is also plotted in the figure. Although a direct comparison is difficult because the real bore front has a finite length (i.e. the locations of the bore front and the height do not coincide), the head height appears to exceed the predicted bore height, whereas the height behind the head appears to be in good agreement with the prediction. The deviation in the

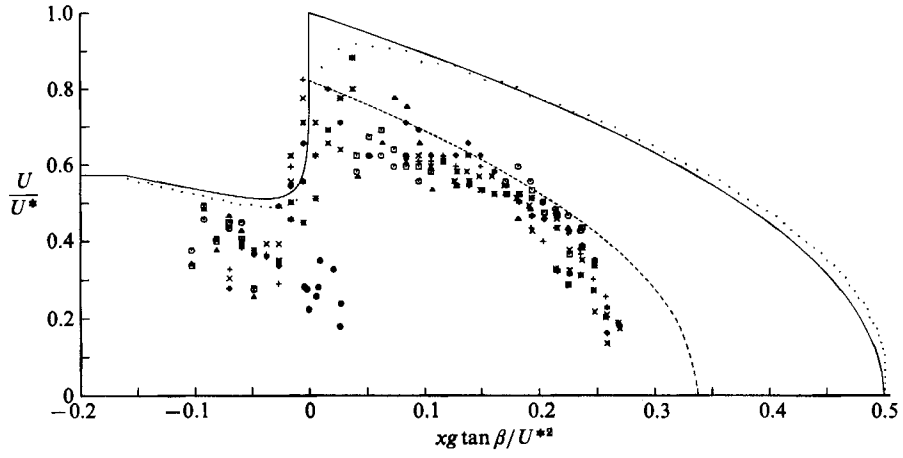

FIGURE 6. Variation of bore and run-up front velocities. Initial Froude number, $F = 1.43$; $U^* = 243$ cm/s; ——, theoretical velocities by (6) and (7); · · · · ·, numerical results; - - - - -, theoretical velocities modified by $0.82\,U^*$. Different symbols denote measured velocity data taken from the repeated experiments and ● is the velocity of the 'bore front', i.e. the motion of f shown in figures 2 and 7.

offshore region (near the beach toe) could be due to transient process in the bore development near the gate. On the other hand, the uniformity of the bore height on the beach provides evidence of the formation of a fully developed bore nearshore even with the limited propagation distance available in the experiments.

The propagation speed, U, of the bore front and the ensuing run-up front were measured by an array of water sensors as described in §2. The data were taken by repeating the experiments with traversing a set of eight water sensors that covers 35 cm propagation distance. The results for initial bore strength $F = 1.43$ are presented in dimensionless form in figure 6 (A scaling parameter, $U^* = 243$ cm/s, is obtained by (6) with the initial condition.) In addition to the analytical prediction by (6), the numerical results are also presented in the figure. The numerical computation used here (based on the Lax–Wendroff numerical scheme) is basically the same as that developed by Hibberd & Peregrine (1979). As shown in figure 6, the numerical result is in good agreement with the analytical result, except that the transition from bore to run-up is smooth in the numerical result owing to the effects of the spatial and temporal discretizations involved in the numerical scheme. This agreement arises from the fact that both solutions are based on the same inviscid governing equations (the shallow-water wave equations, (1) and (2)); the only difference is that energy dissipation in the analytical solution is caused by the jump conditions, (3) and (4), whereas the dissipation in the numerical solution is related to the Lax–Wendroff numerical scheme. Because of the excellent agreement between the analytical and numerical predictions, the experimental results will be compared with the analytical results of (6), but not with the numerical predictions.

In spite of the repeatable bore-generation system described in §2, the propagation velocity data offshore exhibit large scatter in figure 6. This scatter is not measurement errors nor a repeatability problem but is due to the irregularities associated with the bore propagation itself, i.e. a bore front is not smooth and the propagation of the front widely fluctuates. This behaviour was implied in Miller's (1968) experimental data and is shown by Yeh & Mok (1989). Figure 6 also indicates that the bore velocity

offshore, U, decelerates faster than the prediction by (6). Note that this result contradicts the numerical prediction of Svendsen & Madsen's (1984) turbulence model, which is based on the inviscid shallow-water wave theory. On the other hand, a similar discrepancy was found in Miller's (1968) experimental results with the initial Froude number $F = 1.47$; the value of U decelerates to 68% of the velocity measured at the beach toe, which is equivalent to $U/U^* \approx 0.39$ in figure 6. Hence, the faster deceleration of the bore appears to be truly physical but not caused by the particular experimental set-up nor procedure used. In particular, Miller's result is based on a much smaller beach slope (2°) and a longer propagation distance (approximately $65\eta_0$ where η_0 is the bore height offshore in the horizontal-bottom region) than those used in the present study (7.5° and $20\eta_0$, respectively). Furthermore, Miller used a flat vertical piston to generate the bores, whereas the bores in the present study were generated by lifting the gate. Besides the frictional effects and the effects of frequency dispersion, the reason for this discrepancy is not clear. Nonetheless, this compression of bore front as it propagates towards the shore is consistent with the formation of the bore 'head' discussed in connection with figures 4 and 5.

In figure 6, the measured results seem to support qualitatively the occurrence of bore collapse, i.e. a sudden acceleration of the bore propagation is evident from the results. However, the photographic results shown in figure 2 indicate that the actual transition involves momentum exchange between the incident bore and the small wedge-shaped water along the shoreline, but not a genuine bore collapse. (Note that, as discussed in §1, the term 'momentum exchange' is used here to describe the transition process shown in figure 2.) The widely scattered data near the shoreline are due to this momentum exchange process. The acceleration caused by the collided water mass appears to commence earlier than the theoretical bore collapse prediction. Also plotted in figure 6 are the velocity of the 'bore front' during the transition (see figures 2 and 7 for the location of 'bore front', the velocities of which were computed by two consecutive photographs such as those shown in figure 7); because of the momentum exchange process, the location of the bore front lags behind the run-up water front. The result indicates that the bore front velocity reduces during the transition process.

During the run-up process, the propagation velocity is always smaller than the prediction. The run-up front velocities predicted by (7), are modified by using the measured maximum velocity ($0.82U^*$) at the shoreline and presented by the broken line in figure 6. The measured values seem to be in fairly good agreement with the modified prediction. However, although the data are widely scattered, a careful observation of figure 6 reveals that the run-up front decelerates slower than the prediction in the region of $xg\tan\beta/U^{*2} = 0.1$ to 0.2 ($x = 45$–90 cm). This trend is not unique to the bore shown in figure 6 but also appears in the experimental results for other initial bore strengths (this will be shown in figure 8). Owing to the viscous effect present, the bore front should have decelerated faster than the prediction of the inviscid theory. (Based on the assumption of a thin run-up water layer, the theory predicts that the run-up motion is governed by the gravity force only.) Hence, this adverse trend suggests that gravity is not the only force dominant but that the pressure force is also important during the early stage of the run-up. Considering the transition process at the shoreline, the run-up motion is initiated by 'pushing' the water mass. This momentum exchange process is not instantaneous but rather gradual, and the run-up motion forms a thick layer of flow. Hence, the driving force for the run-up motion appears to be the pressure gradient existing during the

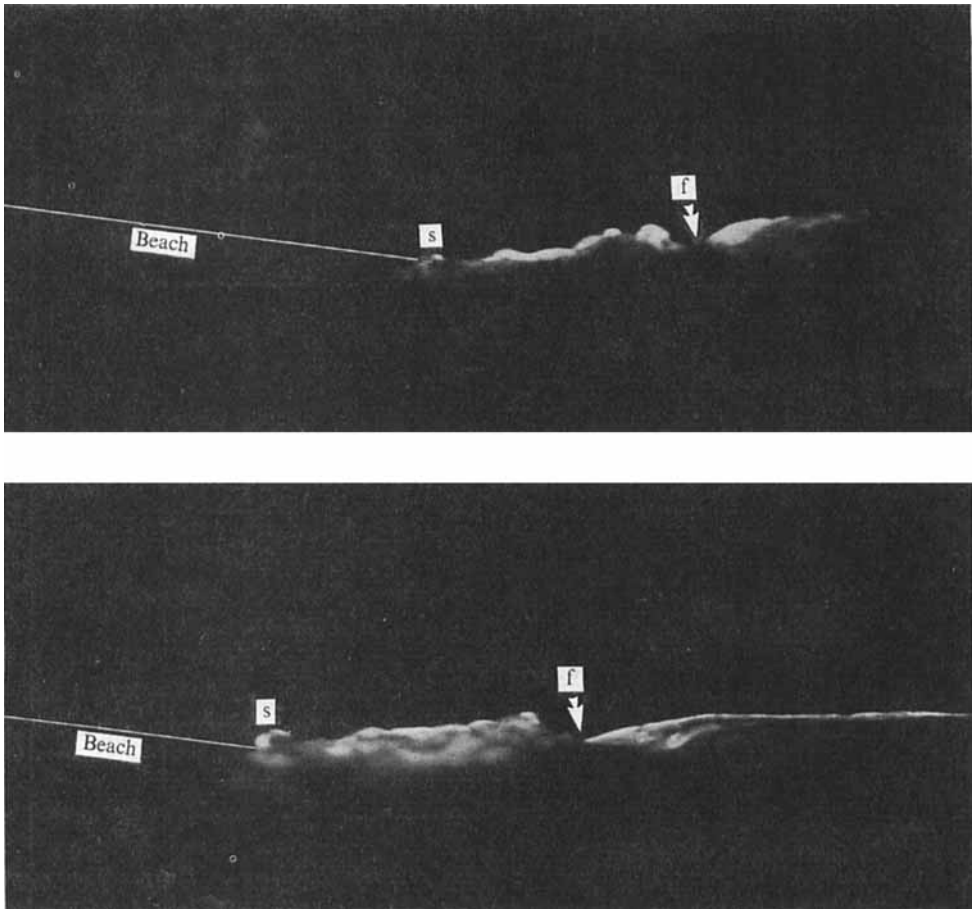

FIGURE 7. Initiation of run-up generated by the initial Froude number, $F = 1.43$. Time difference between (*a*) and (*b*) is 0.103 s. f, bore front; s, run-up wave tip.

transition. (Note that a thin layer of flow could not be influenced by the pressure gradient, as discussed by Ho *et al.* (1963). A thick turbulent layer of run-up water is evident in the time-sequence photographs shown in figure 7.)

The velocity variations of the bore front and of the run-up front for four different initial bore conditions (the initial Froude number $F = 1.31$ to 1.48) are presented in figure 8. All of the initial bore conditions generate fully developed bores. In figure 8, the data reasonably coincide into one pattern indicating (i) the slower propagation speed offshore than the prediction, (ii) the large scatter near the shoreline, (iii) slower deceleration than the prediction during the earlier stage of the run-up in the region of $x\,g\tan\beta/U^{*2} = 0.1$ *to* 0.2. The results in figure 8 support the discussion of figure 6, i.e. the characterizations we made for figure 6 are valid for the range of (fully developed) bore conditions and not limited to the case with the Froude number, $F = 1.43$. Furthermore, in spite of the different bore and run-up behaviour from the predictions, collapsing all the non-dimensionalized data into a single pattern suggests that the maximum run-up height can be predicted from the initial condition (h_1 and h_0) by the shallow-water wave theory by modifying the value of U^*. Based on direct measurements from the video recordings, measured run-up heights are approxi-

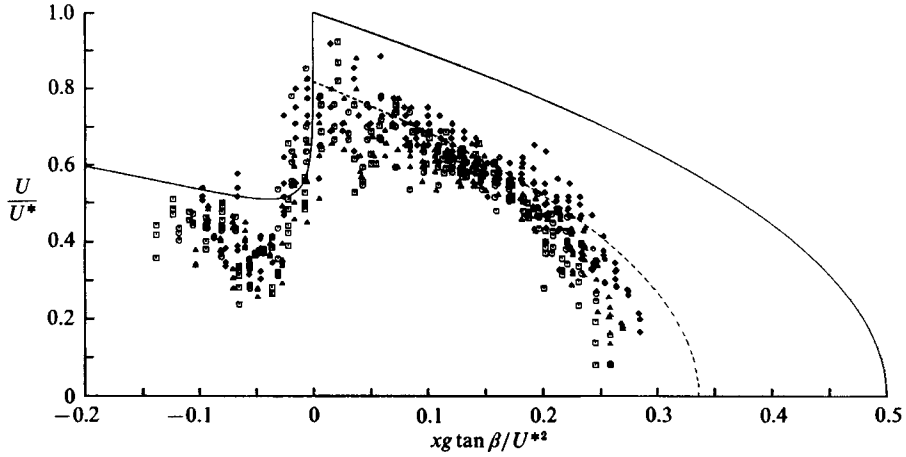

FIGURE 8. Variation of bore and run-up front velocities for various initial bore strengths: □, $F = 1.31$; ○, $F = 1.37$, △, $F = 1.43$; ◇, $F = 1.48$; ——, theoretical velocities by (6) and (7); -----, theoretical velocities modified by 0.82 U^*.

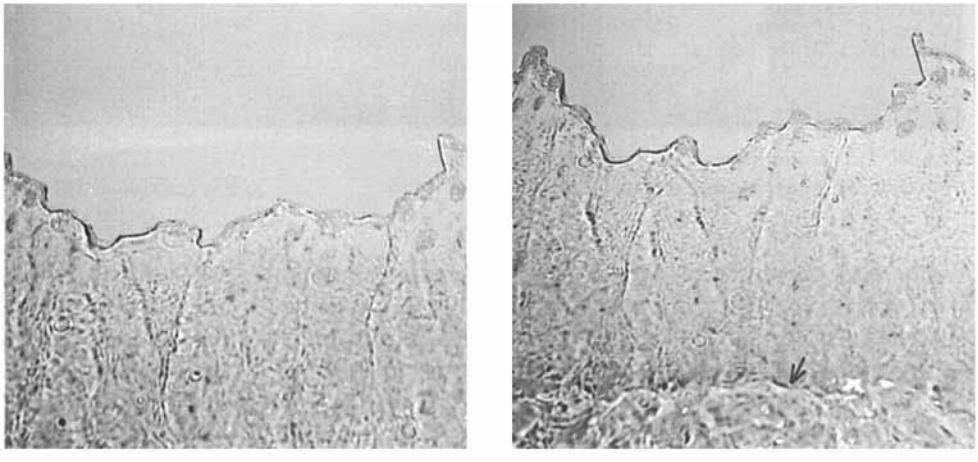

FIGURE 9. Run-up waterline variation near its maximum. Time difference between (*a*) and (*b*) is 0.25 s. Initial Froude number, $F = 1.43$; the arrow in (*b*) identifies the successive run-up motion.

mately 60% of the predicted values, which is equivalent to the reduction of U^* by 77%. Although the beach surface roughness must contribute to the reduction of U^*, the transition process at the shoreline should also be responsible since the transition is not the total bore collapse but rather a gradual transition influenced by the pressure force.

The run-up waterline near its maximum is shown in a sequence of photographs in figure 9. As seen, the water line is not straight, but instead forms distinct 'tongues'. The tongue formations must be due to the air–water–beach contact-line effects. The two major run-up regions near the sidewalls may be caused by three-dimensional effects in the experiment; for example, the sidewall effects cannot be eliminated in the laboratory environment. Figure 9 also shows the formation of complex capillary waves as well as the formation of ridges behind the water line. It may be interpreted

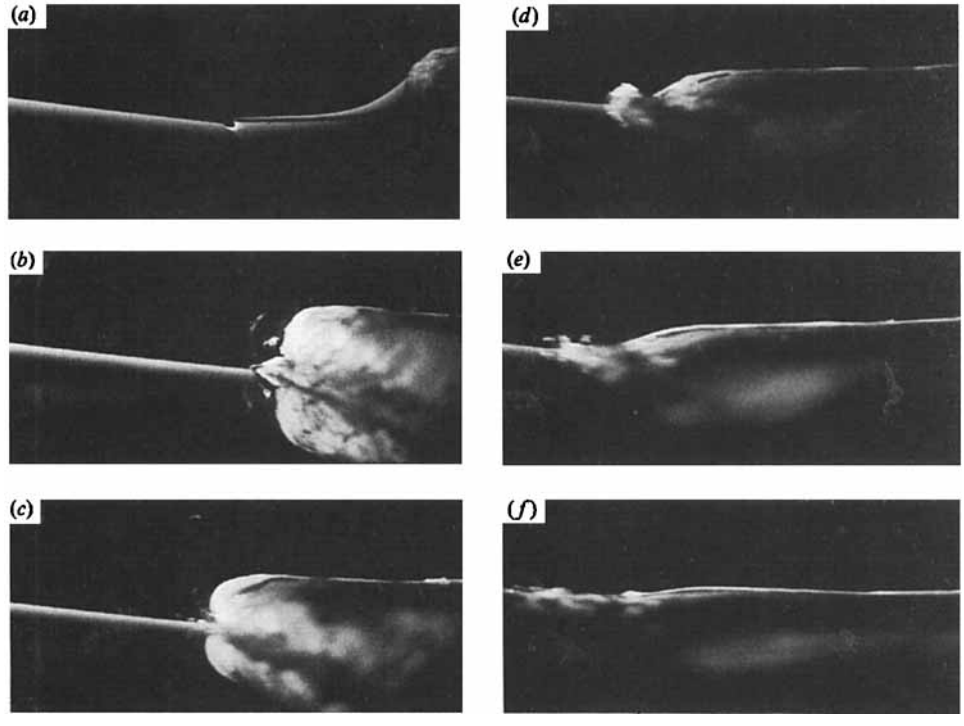

FIGURE 10. Transition process from undular bore to run-up mode. Initial Froude number, $F = 1.18$. (*a*) Bore approaching the shore, (*b–e*) transition, (*f*) run-up (after Yeh & Ghazali 1988).

that the ridge formation is generated by irregularities of the bore front. Turbulent rollers on the bore front are irregular and three-dimensional, and the turbulence is advected onto the beach during the transition process at the shoreline. These irregularities at the shoreline may influence the formation of a run-up water sheet. Also observed is the appearance of the successive run-up waves in the bottom portion of figure 9b. This double structure of the run-up motion must be related to the transition process at the shoreline. This conjecture is supported by figure 7 in which two run-up water masses appear to be formed; the run-up of the pushed-up water mass at the shore is followed by the original bore 'front' motion which was once decelerated during the transition process (figure 6). Turbulence involved in the leading run-up water mass in figure 7 also supports the irregular motion existing near the run-up front. The similar appearance of the waterline and the formation of ridges shown in figure 9 were also observed for other fully developed bores with different initial bore strength with the range of $F = 1.31$ to 1.48.

3.2. *Undular bore*

With the initial condition $h_1/h_0 < 2.0$, the generated bore remains undular at the shoreline although the leading wave is breaking at its crest. The transition process of the undular bore to run-up was analysed experimentally by Yeh & Ghazali (1988). As shown in figure 10 (with $h_0 = 9.75$ cm and $h_1 = 16.75$ cm; $h_1/h_0 = 1.72$ and the Froude number $F = U_0/(gh_0)^{\frac{1}{2}} = 1.18$), the transition process is different from that of a fully developed bore. Instead of the momentum exchange that occurs for a fully developed bore, the front of undular bore overturns directly onto the dry beach

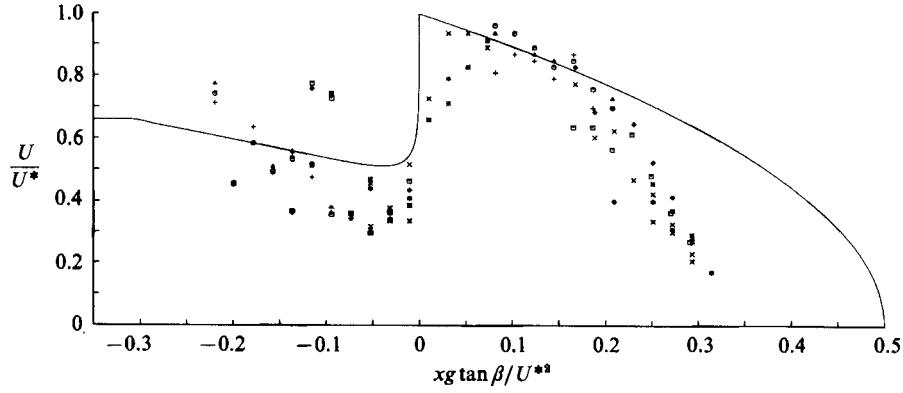

FIGURE 11. Variation of bore and run-up front velocities. Initial Froude number, $F = 1.18$; ——, theoretical velocities by (6) and (7) with $U^* = 175$ cm/s. Different symbols denote measured velocity data taken from the repeated experiments.

surface. The run-up motion then commences with the formation of a thin layer of splash-up water.

The velocity variations of bore and run-up front are shown in figure 11. There is no analytical solution available for an undular bore run-up at the present time, hence we simply use (6) (for a fully developed bore) for the comparison with our experimental data. Figure 11 indicates that the bore velocity offshore, U, decelerates faster than the prediction by (6). However, unlike the results for fully developed bores (figure 8), the acceleration starts at the shoreline rather than an offshore location. The maximum velocity is in good agreement with the predicted value U^* ($= 175$ cm/s), but occurs at the inshore location, $x g \tan \beta/U^{*2} \approx 0.085$ ($x \approx 20$ cm). Note that the substantial discrepancy in the maximum velocity was found between the measured and predicted values for a fully developed bore (figure 8). For the undular bore, no momentum exchange takes place at the shoreline but its front face overturns onto the dry beach surface directly. The entire incident energy is transferred into the kinetic energy of thin fluid layer for the run-up motion just as predicted by theory. This agreement in turn supports the view that the discrepancy in the velocity which appeared for fully developed bores is related to the transition process which is different from that for the undular bore.

Because the run-up motion is initiated by the thin splash-up water layer, the model suggested by Shen & Meyer (1963) should be applicable, i.e. the run-up motion is totally governed by the gravity force and the maximum run-up height is given by (8). (The pressure force cannot play a significant role in a motion of thin layer of fluid.) The results in figure 11, however, indicate that the run-up motion decelerates at a much faster rate than the inviscid prediction. The faster deceleration is explained by the viscous and surface-tension effects, which in turn supports the conjecture that for the fully developed bores shown in figure 8, the pressure force plays a role in the run-up motion since its deceleration is slower than the prediction.

The run-up waterline variation near the maximum run-up is shown in figure 12. Compared to figure 9 for the run-up of a fully developed bore, the 'tongue' formation of the contact line is finer and the run-up water surface is smooth. The run-up water appears to be thin and in agreement with the transition process shown in figure 10. The irregularities (e.g. ridge formations) observed in figure 9 are not present in figure 12. This is because the run-up motion is initiated by overturning a nearly two-

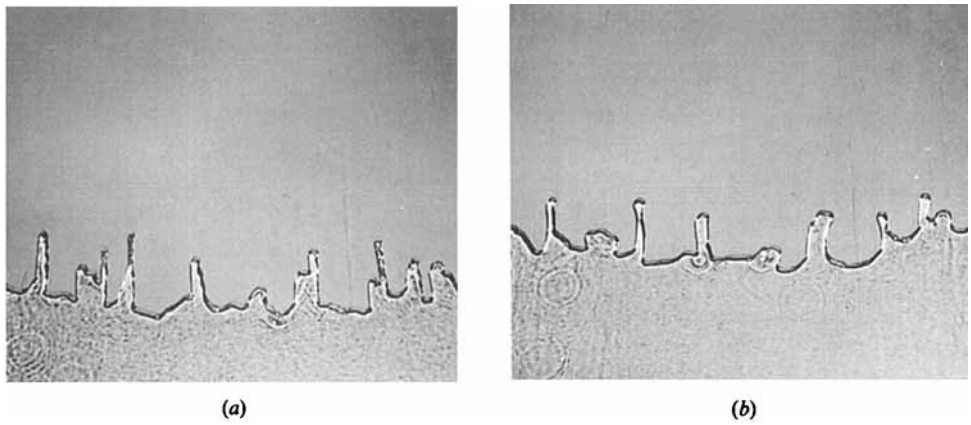

(a) (b)

FIGURE 12. Run-up waterline variation near its maximum. Time difference between (a) and (b) is 0.25 s. Initial Froude number, $F = 1.18$.

dimensional wave and the thin run-up water layer prevents turbulence from advecting towards the run-up front. The behaviour of run-up is evidently different from that of the fully developed bore, and the differences support our conjectures for fully developed bores, i.e. that the formation of ridges in figure 9 is due to irregularities of the driving bore, and the thick run-up water layer is generated by the momentum exchange process at the shoreline.

4. Conclusions

The behaviour of a single bore propagating onto quiescent water on a plane beach and its ensuing run-up motion was investigated experimentally. Bores with a range of initial Froude number, $F = 1.18$ to 1.48, were generated in the wave tank. Based on the experiments described herein, the following conclusions can be drawn.

(i) The speed of bore propagation on a uniformly sloping beach decelerates faster than the inviscid, shallow-water wave prediction. This is consistent with the experimental results provided by Miller (1968) but contradicts the numerical results from the turbulence model of Svendsen & Madsen (1984).

(ii) Although the qualitative behaviour of the propagation during the transition from bore to run-up mode resembles the 'bore collapse' predicted by the theory, the acceleration results from the water 'pushed up' by the momentum exchange process and is not due to the speed of the 'bore front' itself. (For the location of the 'bore front', see figures 2 and 7. The term 'momentum exchange' is used to characterize the transition shown in figure 2.)

(iii) Contrary to the theoretical prediction, the pressure force must play a role in the early stage of run-up motion. The transition process at the shoreline involves 'pushing' a relatively thick layer of water mass; hence, the pressure gradient drives the run-up water initially. (According to the theory, the gravity force dominates the entire run-up motion.)

(iv) Even though discrepancies in the fundamental behaviour of bore motion were found, the maximum run-up height can be predicted by the inviscid theory using a modified (reduced) value of the initial run-up velocity. Besides the friction effect, this reduction of the initial run-up velocity might be related to the transition process; instead of sudden conversion of potential to kinetic energy (as predicted by the

theory), the run-up water is pushed up by the gradual momentum exchange via pressure force.

(v) The motion in the neighbourhood of the run-up waterline was found to be complex. Surface-tension effects, including the air–water–beach contact line and the generation of capillary waves, appear to be important for the complete description of run-up motion in the laboratory environment. The complex flow pattern must be related to irregularities involved in the driving bore; i.e. the bore front formed by surface rollers is irregular, and turbulence advected into the run-up flow also contributes to the formation of a rough run-up water surface.

(vi) A single incident bore generates two successive run-up motions; one is due to the water mass pushed up by the momentum exchange and the other is the original bore motion once it has decelerated during the transition at the shoreline.

(vii) The behaviour of an undular bore is different from that of a fully developed bore. The transition of the undular bore to run-up mode is characterized by overturning the bore front onto the dry beach surface. Consequently, the maximum velocity occurs at the inshore location, and the run-up motion is thin, splash-up water layer. Because of the thin layer run-up, the motion is considered to be governed by the gravity force (just as predicted by the theory) and influenced by the viscous and surface-tension effects. Contrary to the run-up of a fully developed bore, the run-up water surface is smooth because the run-up motion is initiated by the nearly two-dimensional wave.

The authors wish to thank T. McKay of the University of Washington for his assistance in setting up the experimental facility. The work for this paper was supported by the US National Science Foundation Grant no. ECE-8503436 and CES-8715450. Professor D.H.Peregrine, Dr E.D.Cokelet, and referees are thanked for helpful comments.

REFERENCES

HIBBERD, S. & PEREGRINE, D. H. 1979 Surf and run-up on a beach: a uniform bore. *J. Fluid Mech.* **95**, 323–345.

HO, D. V. & MEYER, R. E. 1962 Climb of a bore on a beach. Part 1: Uniform beach slope. *J. Fluid Mech.* **14**, 305–318.

HO, D. V., MEYER, R. E., & SHEN, M. C. 1963 Long surf. *J. Mar. Res.* **21**, 219–232.

KELLER, H. B., LEVINE, D. A. & WHITHAM, G. B. 1960 Motion of a bore over a sloping beach. *J. Fluid Mech.* **7**, 302–316.

MADSEN, P. A. & SVENDSEN, I. A. 1983 Turbulent bores and hydraulic jumps. *J. Fluid Mech.* **129**, 1–25.

MILLER, R. L. 1968. Experimental determination of run-up of undular and fully developed bores. *J. Geophys. Res.* **73**, 4497–4510.

PACKWOOD, A. R. & PEREGRINE, D. H. 1981 Surf and run-up on beaches: models of viscous effects. *Rep.* AM-81-07. University of Bristol. 34 pp.

PEREGRINE, D. H. & SVENDSEN, I. A. 1978 Spilling breakers, bores and hydraulic jumps. *Proc. 16th Conf. Coastal Engng*, pp. 540–550.

SHEN, M. C. & MEYER, R. E. 1963 Climb of a bore on a beach. Part 3. Run-up. *J. Fluid Mech.* **16**, 113–125.

SVENDSEN, I. A. & MADSEN, P. A. 1984 A turbulent bore on a beach. *J. Fluid Mech.* **148**, 73–96.

SVENDSEN, I. A., MADSEN, P. A. & HANSEN, J. B. 1978 Wave characteristics in the surf zone. *Proc. 16th Conf. Coastal Engng*, pp. 520–539.

WHITHAM, G. B. 1958 On the propagation of shock waves through regions of non-uniform area of flow. *J. Fluid Mech.* **4**, 337–360.

YEH, H. H. & GHAZALI, A. 1986 Nearshore behavior of bore on a uniformly sloping beach. *Proc. 20th Conf. Coastal Engng*, pp. 877–888.

YEH, H. H. & GHAZALI, A. 1988 On bore collapse. *J. Geophys. Res.* **93**, 6930–6936.

YEH, H. H. & MOK, K. M. 1989. On turbulence in bores. *Phys. Fluids* (submitted).